Hindawi
Advances in Civil Engineering
Volume 2019, Article ID 4693757, 15 pages
https://doi.org/10.1155/2019/4693757

Research Article

Study on Physical-Mechanical Properties and Microstructure of Expansive Soil Stabilized with Fly Ash and Lime

Sheng-quan Zhou[1,2], **Da-wei Zhou**[1,2], **Yong-fei Zhang**[1,2] and **Wei-jian Wang**[1,2]

[1]*School of Civil Engineering and Architecture, Anhui University of Science and Technology, Huainan 232001, China*
[2]*National Engineering Laboratory for Deep Shaft Construction Technology in Coal Mine, Anhui University of Science and Technology, Huainan 232001, China*

Correspondence should be addressed to Da-wei Zhou; 2997805549@qq.com

Received 22 July 2019; Revised 20 October 2019; Accepted 28 October 2019; Published 14 November 2019

Academic Editor: Claudio Mazzotti

Fly ash and lime have been frequently employed to reduce the swelling potential of expansive soils. Laboratory experiments, scanning electron microscopy (SEM), and X-ray diffraction (XRD) were used in this study to investigate the stabilizing effect of fly ash and lime on expansive soils in the Jianghuai undulating plain area. The comparison was drawn between the variation laws of physical parameters, mechanical properties, microstructure, and mineral composition of expansive soil before and after being stabilized. Experimental results suggest that, after 5% lime is added based on fly ash, the plasticity index of the expansive soil decreases by 64.9%, the free swelling ratio is reduced to about 10%, the unloading swelling ratio is reduced to nearly 4%, and the stabilized soil no longer exhibits the expansive property. The unconfined compressive and tensile strengths of the stabilized soil increase first and then decrease with the rising in fly ash content. After the addition of 5% lime, both the unconfined compressive and tensile strengths increase significantly. The optimum modifier mixture ratio is obtained as 10% fly ash + 5% lime. The SEM images reveal that the microstructures of the stabilized expansive soil vary from an irregular flake-like and flocculent structures to blocky structures, and the soil samples compactness is enhanced. XRD results indicate that quartz is the main component of the stabilized soil. These are the underlying causes of the rise in the strength. The conclusions of this study can be referenced for the engineering design and construction of expansive soil in Jianghuai undulating plain area.

1. Introduction

Expansive soil refers to a type of clay with repeated expansion and shrinkage properties for its moisture variations [1–4]. It is primarily composed of montmorillonite and illite [5–9]. It was not until 1938 that the United States Reclamation Bureau initially discovered the problem caused by expansive soils in a foundation engineering project in Oregon. Since then, engineers have come to realize the damage caused by the expansive soil. Engineering problems caused by expansive soils are repetitive and permanent. Damages to light buildings, foundation pits, and roadbeds usually lead to serious consequences [10–13]. This is because the expansive pressure destroys the stress state and leads to the instability of structures. Therefore, as an important identification, there are many methods to measure the expansive pressure. The traditional methods include direct and indirect measurements. The direct measurement method keeps the volume of soil sample unchanged by applying constraint force in the direction of water absorption and the constraint force is equal to expansive force [14]. The indirect measurement method is carried out by studying the relationship between some parameters (initial moisture content, dry density, liquid and plastic limit, cation exchange capacity, etc.) and the expansive pressure firstly, and then the empirical fitting equation between these parameters and the expansive pressure is established to predict and calculate the expansive pressure [15]. With the development of computer technology, artificial neural network (ANN), support vector machine (SVM), and other artificial intelligence

technologies have also been used in the prediction of parameters like the expansion potential in road geotechnical engineering, which open up a new field for the research of expansive soil [16].

There are two major theories of the expansion and shrinkage mechanisms of expansive soil. One is the crystal swelling theory of clay mineralogy [17], and the other is the diffuse double layer theory of modern colloidal chemistry [18]. Crystal swelling theory states that clay minerals exhibit crystal structures, and flakes are found between the crystal structures. In general, free cations are observed between the flakes. After entering the flakes, the water molecules get combined with the cations to form hydrated ones. The more hydrated the cations, the larger the distance between the flakes will be. Macroscopically, this phenomenon is manifested as soil swelling [19, 20]. Crystal swelling theory interprets expansion mechanism of soils based on the crystal structures, whereas it ignores the adsorption between clay particles. Diffuse double layer theory states that the surface of clay minerals is negatively charged, leading to the formation of an electric field around the soil particles. The hydrated ions and polar water molecules are firmly adsorbed on the surfaces of the particles to form a fixed layer. Outside the fixed layer, the electrostatic attraction is low, and the activities of hydrated ions and polar water molecules are larger than those in the fixed layer, which leads to the formation of a diffusion layer. The thickness of the combined water film between the clay particles increases due to the entry of water molecules, thus widening the spacing between particles. From the macroscopical perspective, this phenomenon is reflected as soil swelling [21].

In recent years, numerous methods of stabilizing expansive soil have been developed by many scholars. Their research results show that cement, lime [22], and fly ash [23] are feasible to reduce the swelling potential of expansive soil. To explore the stabilizing effect of fly ash on expansive soil, Mir et al. [24] highlighted that the increase in the amount of fly ash and stabilizing time led to the decrease in the compression index and the consolidation coefficient. Bose [25] reported that 20% fly ash downregulated the liquid limit of expansive soil by 43%, the plastic limit by 52%, and the plasticity index by 39%. As fly ash content was upregulated, the unconfined compressive strength of the modified expansive soil first increased and then decreased. When the fly ash content reached 20%, both the unconfined compressive strength and the California bearing ratio (CBR value) of the modified expansive soil reached their peaks. The aforementioned studies mostly focused on the comparative study on the expansion index and the mechanical properties before and after soil was modified. Their results all implied that suitable fly ash can increase the unconfined compressive strength. However, these studies lacked the analysis of the mechanism of stabilizing expansive soil from the microstructure.

For the stabilizing effect of lime on expansive soil, Sabat [26] added 7% lime to the quarry waste and expansive soil mixture, and the stability of expansive soil was enhanced. The liquid limit, the plastic limit, and plasticity index decreased from 60% to 25.2%, 32% to 22.8%, and 28% to 2.4%, respectively. The optimum moisture content was upregulated with the lime content, and the maximum dry density was downregulated as lime content increased. However, lime exhibited poor stability as a modifier alone. This defect is crucial to engineering applications [27]. Wang et al. [28] adopted lime and cetyltrimethylammonium bromide (CTMAB) as modifiers to stabilize expansive soils in Hefei area. Besides, the scanning electron microscopy (SEM) was used to explain the mechanism of cation-modified expansive soil from the perspective of microscopic morphology. However, the application cost, environmental protection and other factors of CTMAB as a chemical reagent in engineering require further studies.

Some scholars studied the combined effect of fly ash and lime on expansive soil stabilization. Zha et al. [29] studied the free swelling ratio, the unloading swelling ratio, and the expansion force of expansive soils combined with small amounts of lime and fly ash. Their results showed that, under the same fly ash content, these indicators decreased as more lime was added (0%, 1%, 2%, and 3% in sequence), suggesting that a small amount of lime combined with fly ash can significantly inhibit the expansion and contraction of expansive soil. Sivapullaiah and Jha [30] studied the microscopic mechanism of lime and fly ash by improving expansive soil. They concluded that the variation of soil strength with stabilizing time was primarily attributed to cation exchange and flocculation. This process helped solidified soil particles to be combined with the cement compound. Thus, the soil strength was enhanced.

Besides the common modifiers such as lime and fly ash, some advanced methods like alkali activation method [31] and biological method [32] also have been studied. Each method has its applicable scope. In engineering practice, the best method should be selected after comprehensive consideration of its construction difficulty, environmental effect, project cost, and other factors.

Based on the engineering background in the Jianghuai undulating plain area, this study aims to explore the variation laws of expansive potential, mechanical properties, microstructure, and mineral composition of expansive soil stabilized by fly ash and lime and then to assess the stabilizing effect. The rest of this research is organized as follows. In Section 2, the materials used in the experiment and the different mix proportions of modifier are described, and the corresponding experiment ideas and actual operation procedure are presented. In Section 3, the experiment data are combined to analyze the experiment results in detail. In Section 4, the full text is summarized, and the conclusions are drawn.

2. Methodology

2.1. Experiment Materials

2.1.1. Plain Soil. The expansive soil employed in the experiment was taken from a construction site in Shannan New District, Huainan City. This area belongs to Jianghuai wave plain, where expansive soil distributes widely. The soil sample was 2–3 meters deep. To take out the soil sample, the

weathered soil was excavated first. The undisturbed soil was yellowish brown and hard. The physical parameters of the soil sample are listed in Table 1, and the relevant classification indicators of the expansive soil are listed in Table 2.

2.1.2. Fly Ash and Lime. XRD patterns of fly ash (F) and lime (L) are given in Figure 1. It is suggested that the fly ash is primarily composed of quartz and mullite, while lime mostly contains portlandite and vanadium selenide.

2.2. Test Procedure

2.2.1. Physical Properties. The plasticity index refers to the difference between the liquid limit and plastic limit, indicating the soil's water content range in the plastic state. The plasticity index is a vital indicator commonly used to assess the swelling potential of expansive soils [33–35]. During the measurement of plasticity index, the undisturbed soil was placed in an oven for 24 h to be dried, pulverized, and screened out through a 0.5 mm sieve. The soil was split into two groups. In the first group, fly ash was added. The contents of fly ash were 0%, 5%, 10%, 15%, 20%, 25%, and 30% (mass ratio to dry soil), and seven samples were examined. In the second group, 5% lime (mass ratio to dry soil) was added to each sample based on the first group. A total of 25% water was added to each sample, and the liquid and plastic limits of soil were measured after the soil was stabilized for 48 h. The liquid and plastic limits of the two groups of soil samples were measured using the liquid-plastic limit combined method. Lastly, the water content was plotted on the abscissa, and the fall depth of the cone was plotted on the ordinate. The relationship curve was drawn on the double logarithmic coordinate paper. The water content corresponding to the sinking depth of 17 mm was the liquid limit, and the water content corresponding to the sinking depth of 2 mm was the plastic limit. The value was expressed as percentage, which was accurate to 0.1.

The free swelling ratio refers to the ratio between the increased volume expanded in water and the original volume of the artificially prepared dried soil samples. Soil samples with the same mix proportion as mentioned were dried, crushed, and then screened out through a 0.5 mm sieve. The free swelling ratio of each soil sample was measured by using a PZL-1 type swelling ratio tester and a 50 ml measuring cylinder with a minimum scale of 1 ml. 30 ml pure water and 5 ml analytical NaCl solution at a concentration of 5% (to accelerate the precipitation of soil particles) were added to the measuring cylinder, and the soil sample was poured into the measuring cylinder and then stirred evenly. The measuring cylinder wall was rinsed with water until the volume of solution reached 50 ml. Observing the volume of soil samples after settling and stabilizing, the calculation formula of free swelling ratio is expressed as follows:

$$\delta_{ef} = \frac{V - V_0}{V_0} \times 100\%, \quad (1)$$

where δ_{ef} denotes the free swelling ratio, accurate to 0.1%, V is the volume of the soil expanded and stabilized in the measuring cylinder, mL, and V_0 is the volume of dry soil, 10 mL.

The unloading swelling ratio refers to the ratio between the expanded volume for only one-way water absorption under the condition of lateral limit without loading and the original volume of the soil sample. Likewise, soil samples with the same mix proportion as mentioned were dried, crushed, and then screened out through a 0.5 mm sieve. A WZ-2 dilatometer was employed to measure the unloading swelling ratio of each soil sample. Cylinder samples with a diameter of 61.8 mm and a height of 20 mm were prepared. Samples were put into the WZ-2 dilatometer with dial gauge accurate to 0.01 mm, water was filled into the container from the bottom to the top, and the water surface was kept 5 mm above the surface of the sample. The data of dial gauge were recorded until the difference was below 0.01 mm. The test diagram is given in Figure 2, and the formula of unloading swelling ratio is written as

$$\delta_e = \frac{Z_1 - Z_0}{h_0} \times 100\%, \quad (2)$$

where δ_e denotes the unloading swelling ratio at time t, %; Z_1 is the dial gauge data at time t, mm; Z_0 is the original data of the dial gauge, mm; and h_0 is the original height of the samples.

The test procedures were performed rigorously following the GB/T 50123 -- 1999 Standard for Soil Test Method [36].

2.2.2. Mechanical Properties. A total of 7 samples with different mix proportions (plain soil, 10% F, 20% F, 30% F, 10% F + 5% L, 20% F + 5% L, and 30% F + 5% L) were used to test the mechanical properties of the stabilized soil. Cylinder samples with a diameter of 50 mm and a height of 100 mm were used for unconfined compressive strength test and cylinder samples with a diameter of 50 mm and a height of 25 mm were used for the Brazilian splitting test. All samples were kept with the moisture content of 25%. The unconfined compressive strength and Brazilian splitting tests were performed using a UTM4204 universal test machine, and the loading rates were 2 mm/min and 1 mm/min, respectively.

Four parallel tests were performed for each test. To evaluate the regularity of test data, Cv (coefficient of variation) in statistics was employed to measure the dispersion degree of data, which is expressed as

$$C_v = \frac{SD}{MN} \times 100\%, \quad (3)$$

where SD denotes the standard deviation and MN is the mean value.

2.2.3. Microstructure and Mineral Composition. The plain soil, 10% F, and 10% F + 5% L-modified soil were taken as three groups of representative soil samples to analyze microstructure and mineral composition. Under a Flex-SEM1000 machine, the microstructures of the plain soil, 10% F, and 10% F + 5% L-modified soil were investigated. Before the SEM test, the soil sample was polished and then plated with gold for 120 s to enhance its conductivity. The

Table 1: Physical parameters of expansive soil.

Moisture content w (%)	Density (ρ/g/cm^3)	Dry density (ρ_d/g/cm^3)	Specific gravity (Gs)	Saturability, Sr (%)	Porosity, n (%)	Void ratio e
24.1	1.98	1.60	2.73	92.7	41.5	0.711

Table 2: Classification indicators of expansive soil.

Indicator	Swelling potential level		
	Weak	Moderate	Strong
Liquid limit (%)	40–50	50–70	>70
Plasticity index	18–25	25–35	>35
Free swelling ratio (%)	40–65	65–90	>90
Total ratio of swelling-shrinkage (%)	0.7–2.0	2.0–4.0	>4.0

acceleration voltage of SEM analysis was set to 10 kV. When the XRD test was performed, the soil sample was placed on the stage following the corresponding operating procedures. The scanning angle range was set as 3° to 70°, and the XRD diffraction peak spectrum of each sample was characterized. After the search conditions were set, the corresponding test data were imported into Jade 6.5, and the phase was analyzed.

3. Result Analysis and Discussion

3.1. Analysis of Physical Properties

3.1.1. Liquid Limit, Plastic Limit, and Plasticity Index Variation Laws. The variation laws of liquid limit (LL), plastic limit (PL), and plasticity index (PI) of pure fly ash-modified soil and fly ash-lime combined modified soil are shown in Figure 3. Under the condition of pure fly ash, the LL of the modified expansive soil gradually decreases with the rising percentage of fly ash. The LL of expansive soil is 48.26% under the fly ash content of 0% (plain soil). When the fly ash content is upregulated to 30%, the LL reduces to 43.07% and decreased by 10.8%. The PL of the modified expansive soil rises gradually with the fly ash percentage. The PL is upregulated from 23.35% (plain soil) to 26.51% (30% F added), and the PL increased by 13.5%. The variation laws of LL and PL lead to a significant decrease to the PI of the modified soil, from 24.91 (plain soil) to 17.4 (25% F added) and 16.58 (30% F added). The PI indicates the moisture content range of soil in the plastic state. When the PI decreases, the moisture content range for soil in the plastic state is reduced. This leads to a decreasing content of bound water and clay minerals (montmorillonite mainly) in the soil, thereby reducing the soil's characteristics of water absorption and expansion. According to Table 2, when the PI is less than 18, the soil sample is no longer expansive. Therefore, when the content of pure fly ash exceeds 25%, the soil sample does not belong to expansive soil.

After the addition of lime, the variation of the LL of expansive soil is slightly affected. The LL of the modified soil is reduced from the initial 48.26% to the final 45.11%, which only decreases by 6.5%. The PL of the modified soil increases from 23.35% (plain soil) to 36.37% (30% F + 5% L added), and the increase rate reaches 55.8%. At the addition of 5% F + 5% L, the PI drops significantly to 14.16 (less than 18) and the PI decreases to the lowest value of 8.74 at 30% F + 5% L content. Therefore, after the addition of 5% lime on the basis of fly ash, all the soil samples no longer belong to expansive soil. Experimental data indicate that adding lime on the basis of fly ash can significantly reduce the swelling property of soil.

The diffuse double layer theory states that, when the water molecules and cations in the fixed layer and diffusion layer distribute close to the surfaces of the soil particles, the arrangement will be tidy and tight and mobility will be low. The strongly bound water represents the water in the fixed layer, and the weakly bound water corresponds to the water in the diffusion layer. The thickness of water film of the diffusion layer significantly affects the engineering properties of the clay. For the thickness of the diffusion layer is large, the plasticity of the soil is high and expansion and contraction are strong. Lime and fly ash contain numerous high-valent cations, and the diffusion layer is thinned with the rising in the concentration of high-valent cations in the diffusion layer to reduce the PI and swelling potential of the soil.

3.1.2. Free Swelling Ratio Variation Laws. The comparison of the two groups of experimental free swelling ratio data is drawn in Figure 4. The free swelling ratio decreases gradually from 59.4% of plain soil to the final 32.1% with the rise in fly ash content in the first group (0% L), marking a decrease by 46%. When the content of fly ash reaches 20%, the free swelling ratio of the modified soil is 35.3%, less than 40%, and it is speculated that the modified soil did not belong to the expansive soil. After the addition of 5% lime in the second group (5% L), the free swelling ratio drops sharply to approximately 10% and then remains stable. The free swelling ratio no longer decreases as fly ash content rises.

3.1.3. Unloading Swelling Ratio Variation Laws. Figure 5 shows the relationship among the unloading swelling ratios of three typical soil samples (plain soil, 30% F-modified soil, and 10% F + 5% L-modified soil) over time. It is suggested that the soil in the first 50 minutes is in a rapid swelling phase, and most of the volume swelling is completed in this period. With the addition of fly ash and lime, the initial unloading swelling ratio decreases significantly. The unloading swelling ratio of the soil samples slowly increases over time until they are stabilized.

Figure 6 shows the variation of the unloading swelling ratios of the two group soil samples. When the first group is blended with 5% fly ash, the unloading swelling ratio of the soil samples significantly decreases from 13.13% to 7.38%.

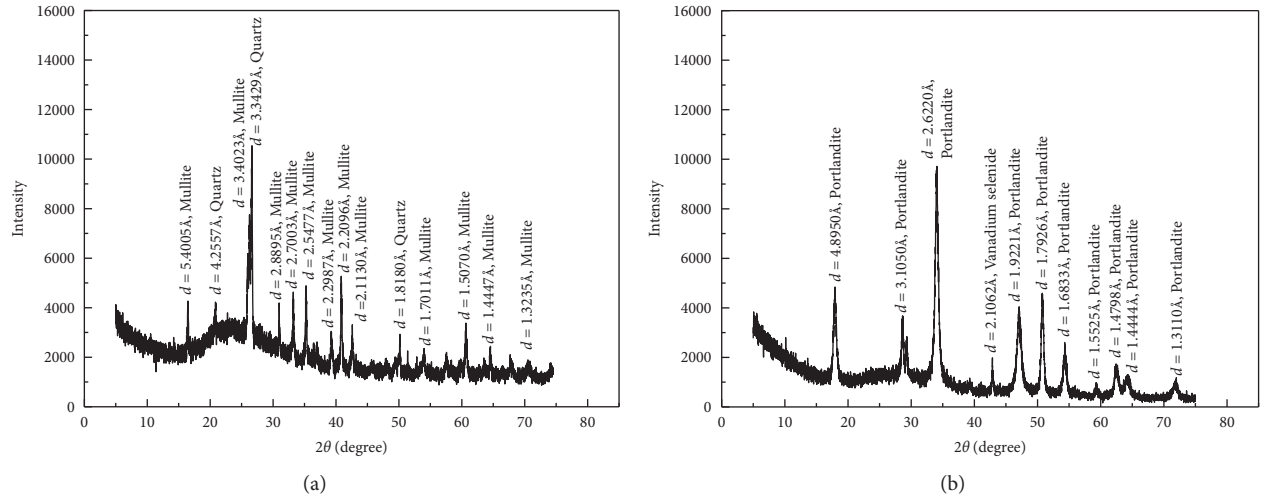

Figure 1: XRD patterns of (a) fly ash and (b) lime.

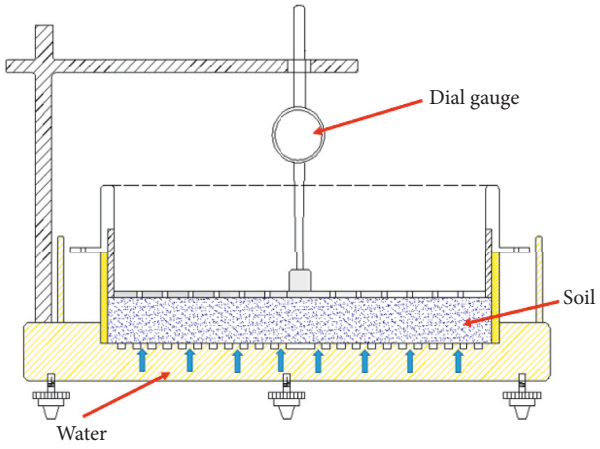

Figure 2: The diagram of unloading swelling ratio test.

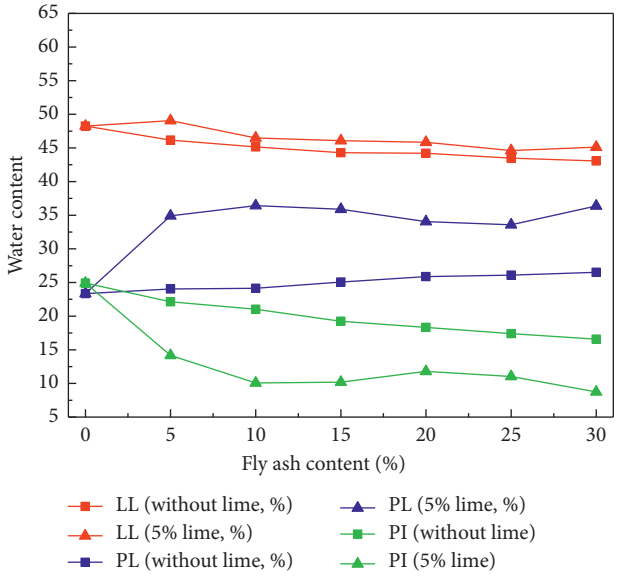

Figure 3: Variation laws of LL, PL, and PI under different fly ash and lime content.

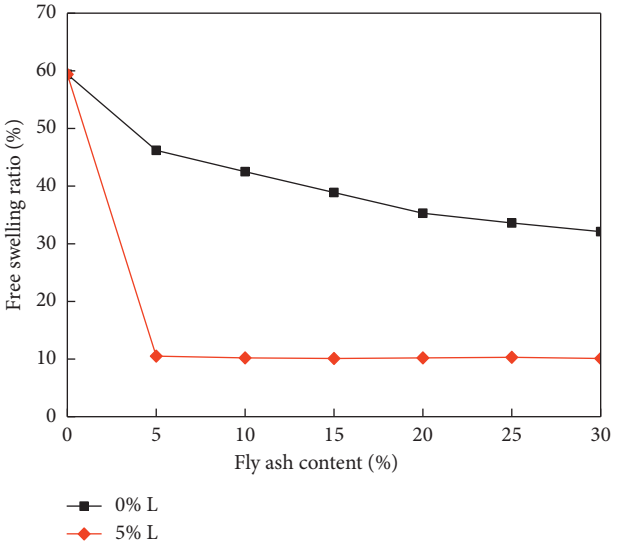

Figure 4: Variation laws of free swelling ratio under different fly ash and lime contents.

Afterwards, it shows a slow fluctuation decline and finally reaches 5.88%. After the addition of 5% lime in the second group, the unloading swelling ratio of the soil samples is downregulated rapidly and reaches a minimum of 4% when 10% F and 5% L are added. According to the test results, when 5% lime is added with fly ash, the unloading swelling ratio decreases significantly.

3.2. Analysis of Mechanical Properties

3.2.1. Unconfined Compressive Strength Variation Laws. Figure 7 shows the stress-strain relationship between plain soil and soil stabilized by fly ash and lime with different mix proportions. It is suggested that the stress-strain curves of plain soil and pure fly ash stabilized soil are obviously split into three stages (including the elastic stage, the plastic stage and the failure stage). In the plastic stage, when the plastic

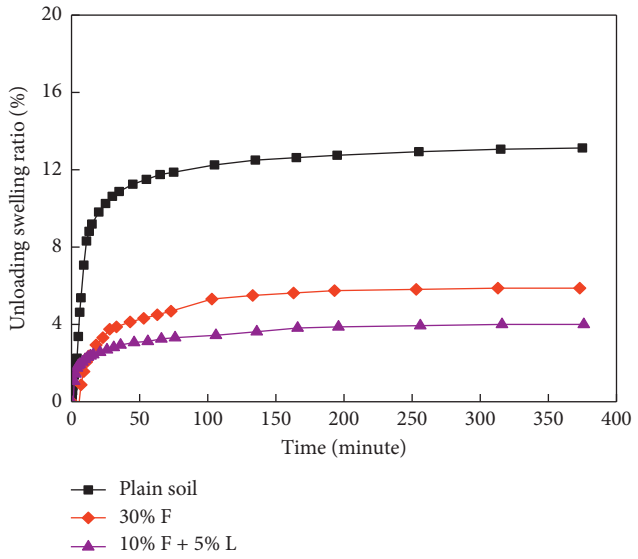

Figure 5: Variation laws of unloading swelling ratio of modified expansive soil over time.

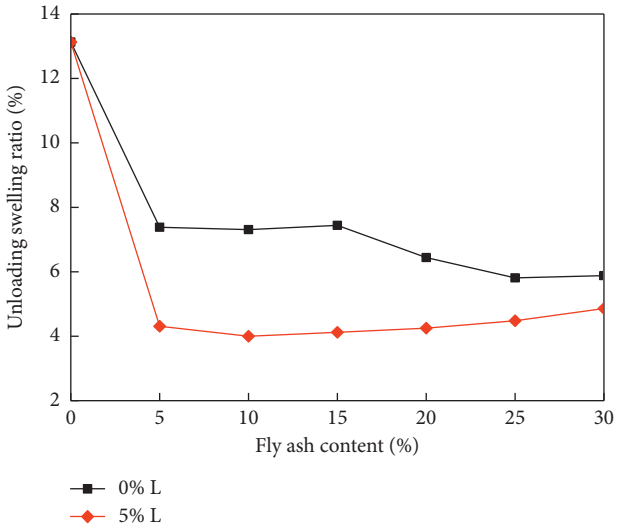

Figure 6: Variation laws of unloading swelling ratio under different fly ash and lime contents.

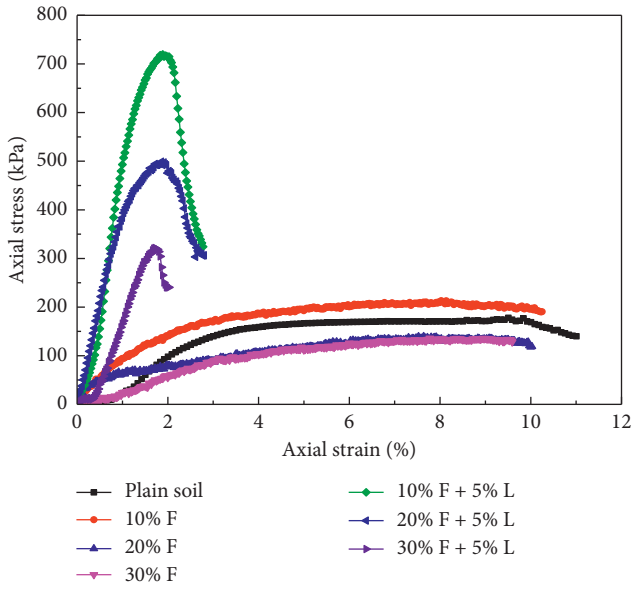

Figure 7: Stress-strain curves of stabilized soil under different mix proportions (7 days).

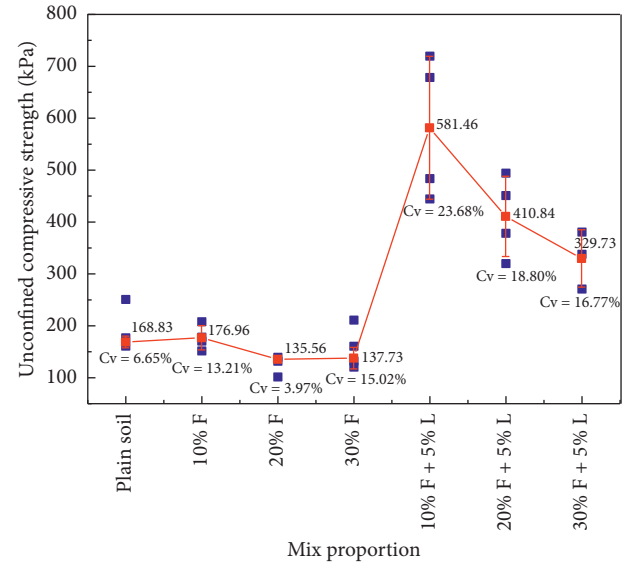

Figure 8: Unconfined compressive strength curve of stabilized soil (7 days).

strain ranges from 4% to 10%, the stress is almost unchanged and an obvious yield platform appears. After the addition of lime, the variation laws of stress and strain of the stabilized soil are obviously different, only for two stages (the elastic stage and the failure stage). The unconfined compressive strength decreases immediately after reaching the peak, exhibiting obvious brittle failure.

Figures 8 and 9 show the unconfined compressive strength variation laws of stabilized soils with different mix proportions under 7 and 28 days of stabilizing, respectively. It is suggested that the variation laws of unconfined compressive strength under different stabilizing time show a consistency. When fly ash is added separately, the unconfined compressive strength of stabilized soil increases first and then decreases as fly ash content is upregulated. When 10% F is added, the strength of the stabilized soil reaches its peak value, 176.96 kPa (7 days) and 588.00 kPa (28 days), respectively. The strengths of 20% F and 30% F stabilized soils (135.56 kPa, 137.73 kPa, 7 days; 396.75 kPa, 360.20 kPa, 28 days) decrease compared with those of plain soil (168.83 kPa, 7 days; 473.25 kPa, 28 days). This is because the fly ash exhibits very low internal friction angle and cohesion, and its engineering properties are similar to those of silty soil. The excess unhydrated fly ash particles reduce the strength of the system. It can be concluded that after the fly ash content reaches over 10%, the excess fly ash negatively

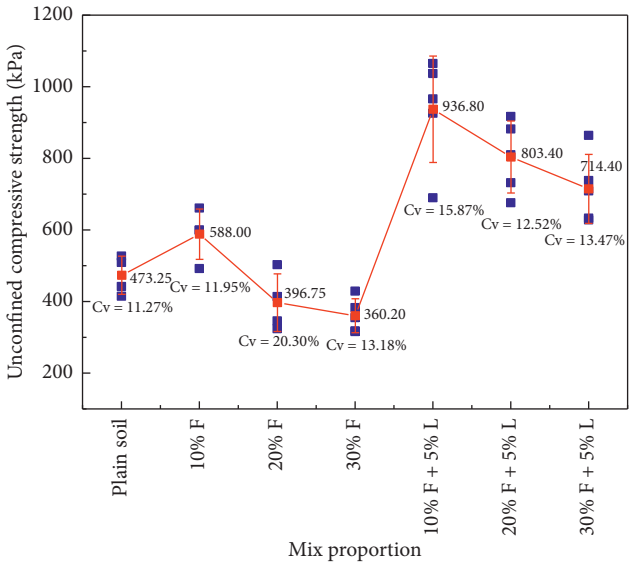

Figure 9: Unconfined compressive strength curve of stabilized soil (28 days).

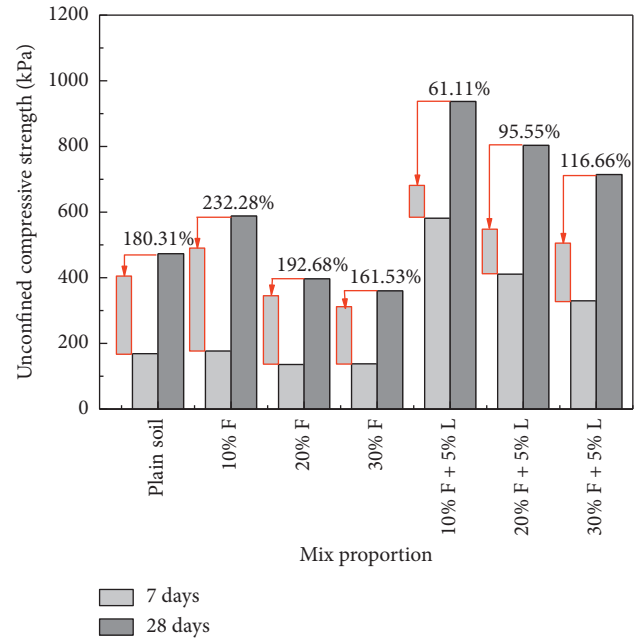

Figure 10: Variation laws of unconfined compressive strength with stabilizing time.

affects the compressive strength of the stabilized soil, and there is an optimal value of fly ash content around 10%.

After the addition of lime based on the fly ash modifier, the compressive strength of the stabilized soil significantly increases. The test data show that, under the condition of 10% F + 5%, the strength of the stabilized soil is the highest, 581.46 kPa (7 days) and 936.80 kPa (28 days), respectively. This is because lime hydration produces more Ca^{2+}, which promotes the ion exchange of the system and pozzolanic reaction, and produces more cementing materials, thus enhancing the strength.

To analyze the effect of stabilizing time on unconfined compressive strength, Figure 10 shows the variation laws of unconfined compressive strength under the stabilizing time of 7 days and 28 days. It is suggested that, after the addition of pure fly ash, the strength of the sample increases significantly in 28 days by 232.28%, 192.68%, and 161.53%, respectively, suggesting that the hydration reaction of fly ash takes a long time. After the addition of lime, the strength of samples increased by 61.11%, 95.55%, and 116.66%, respectively. The strength is enhanced in a relatively slow manner, revealing that the early strength of lime-stabilized soil has already reached a high value, and lime has a significant effect on the early strength.

To further study the failure patterns, the failure strain of soil samples stabilizing for 7 days and 28 days is summarized in Figures 11 and 12. With the rise in fly ash content, the failure strain decreases from 9.64% to 6.49% (7 days) and 5.82% to 5.10% (28 days), respectively. This is because fly ash is similar to silty soil and its plasticity is lower than that of plain soil, thus leading to the reduction of plasticity of stabilized soil. After the addition of lime, the failure strain is significantly reduced, also suggesting that lime promotes the pozzolanic reaction to some extent, resulting in more strong and brittle cementing materials. Figure 13 shows the variation laws of failure strain with stabilizing age. For plain soil

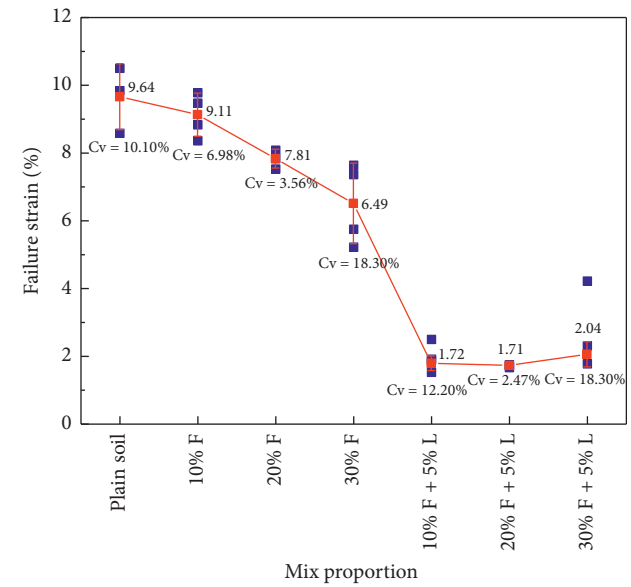

Figure 11: Unconfined compressive failure strain curve of stabilized soil (7 days).

and pure fly ash stabilized soil, the plasticity is gradually downregulated with the rise in the stabilizing age. Accordingly, the failure strain can reflect the completion degree of the chemical reaction in the stabilized soil system to some extent. It is noteworthy that, after the addition of 5% L, the 28-day failure strain increases conversely (Figure 13). Combined with Figure 10, it is suggested that, under the age of 28 days, the strength and failure strain of fly ash-lime combined stabilized soil all increase, so the elastic modulus of stabilized soil is relatively stable. This figure reveals that

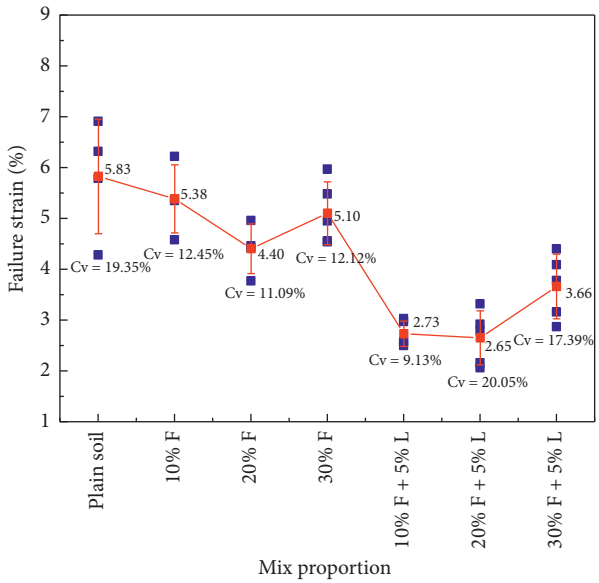

FIGURE 12: Unconfined compressive failure strain curve of stabilized soil (28 days).

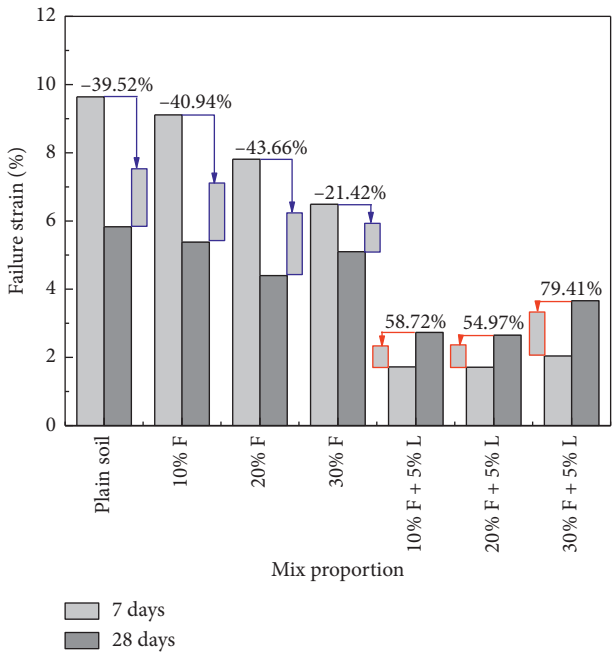

FIGURE 13: Variation laws of unconfined compressive failure with stabilizing time.

the hydration reaction rate of the stabilized soil is faster in the early stage after adding lime and remains stable after that. Thus, lime helps upregulate the rate of early hydration reaction.

3.2.2. Brazilian Splitting Strength Variation Laws. The tensile strength of soil samples measured in the Brazilian splitting test can be calculated indirectly by the following formula:

$$\sigma_t = \frac{2P}{\pi Dt}, \tag{4}$$

where σ_t denotes the indirect tensile strength of soil samples, P is the failure loading, and D and t are the diameter and thickness of samples, respectively. When calculating indirect tensile strength using the formula, two basic assumptions should be satisfied: (1) samples are homogeneous and isotropic material; (2) the macroscopic cracks caused by the failure of the sample start from the central point of the disk. Tavallali and Vervoort [37, 38] found that the macroscopic cracks formed on the disk surface were primarily related to the following three typical failure mechanisms (Figure 14). During the test, it was observed that the through-crack of the sample was generated from the central position first and then gradually expanded to the upper and lower end surfaces with the increase of loading, exhibiting a typical tensile failure. Thus, the test is consistent with the basic assumption of Brazilian splitting test strength calculation formula. The final failure patterns of samples are illustrated in Figure 15.

The stress-strain curve of the Brazilian splitting test is plotted in Figure 16. It is suggested that the splitting process of plain soil exhibits an obvious stress platform stage. After adding fly ash only, there is a small range of stress drop with the rise in the strain, whereas it still has residual strength. After the addition of 5% lime based on fly ash, the tensile strength of the samples is significantly upregulated and immediately downregulated after the peak strength reaches. There is no corresponding residual strength, exhibiting obvious brittle failure.

Figures 17 and 18 give the curves of strength and failure strain variations of samples with different mix proportions. The variation law of Brazil splitting strength curve is consistent with that of the compressive strength, and the tensile strength first increases and then decreases as fly ash content is upregulated. However, the difference is that the peak tensile strength (125.44 kPa) appears at 20% F when pure fly ash is added. After the addition of lime, the tensile strength of the stabilized soil increases significantly. Under the condition of 10% F + 5% L, the tensile strength reaches the peak value (342.38 kPa). The failure strain of Brazilian splitting test first decreases and then increases with the addition of modifiers under different mix proportions, reaching the lowest value (2.83%) under 10% F + 5% L.

It is concluded after comprehensive analysis of unconfined compressive and splitting tests that, under the condition of pure fly ash, fly ash content between 10% and 20% is the optimal mix proportion. In the fly ash and lime combined improvement system, 10% F + 5% L is the optimal mix proportion. This is because more Ca^{2+} is generated after lime hydration, and the positive charge of Ca^{2+} balances the negative charge on the surface of clay mineral particles, so the the plasticity index is downregulated and the expansibility of expansive soil is reduced. Furthermore, the cement produced by hydration of lime also enhances the strength of soil.

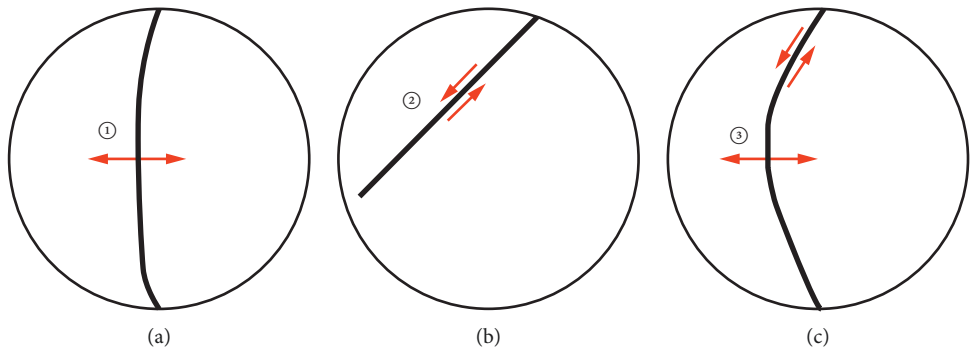

Figure 14: Schematic diagram of three typical failure mechanisms [39]: (a) tensile failure; (b) shearing failure; (c) tensile-shearing composite failure.

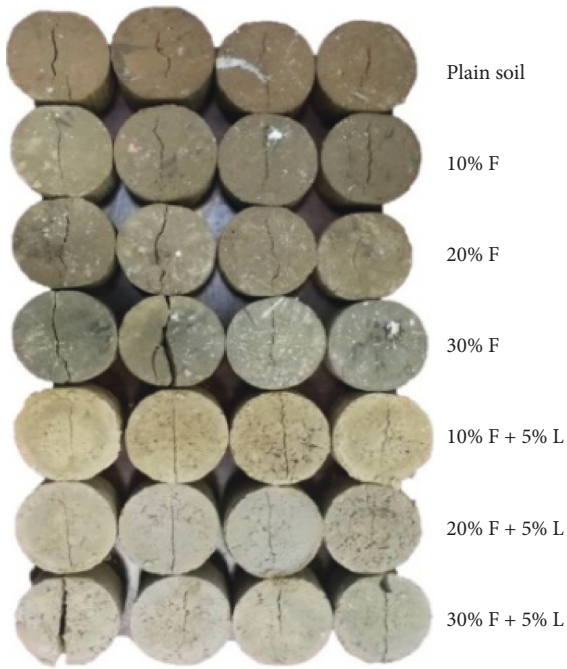

Figure 15: Failure patterns of soil samples.

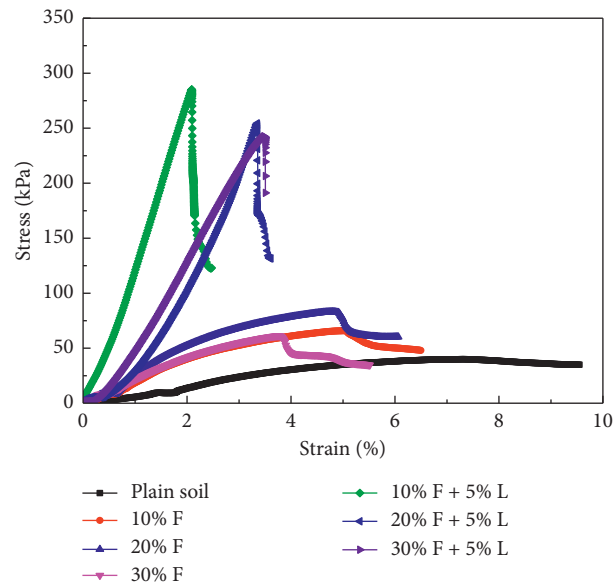

Figure 16: Stress-strain curves of the Brazilian splitting test.

3.3. Analysis of Microstructure and Mineral Composition

3.3.1. SEM Results. Figure 19 gives the SEM images of plain soil to study the microscopic morphology of the expansive soil before and after being stabilized. The surface particles of the expansive soil before the modification are loose, exhibiting obvious pores and cracks, thereby forming water passages. There is obvious flocculent substance between the fissure passages. By magnifying the SEM image, the clay particles exhibit obvious flake or fine flocculent structures (montmorillonite mainly). These irregular structures expand the specific surface area of the soil particles. The ability for water to interact with the soil particles is strong, and the soils absorb considerable water when contacting water. Subsequently, significant expansion is observed.

The microscopic morphology of expansive soil modified by 10% fly ash is shown in Figure 20. The structures of the modified soil are more compact than the plain soil, and

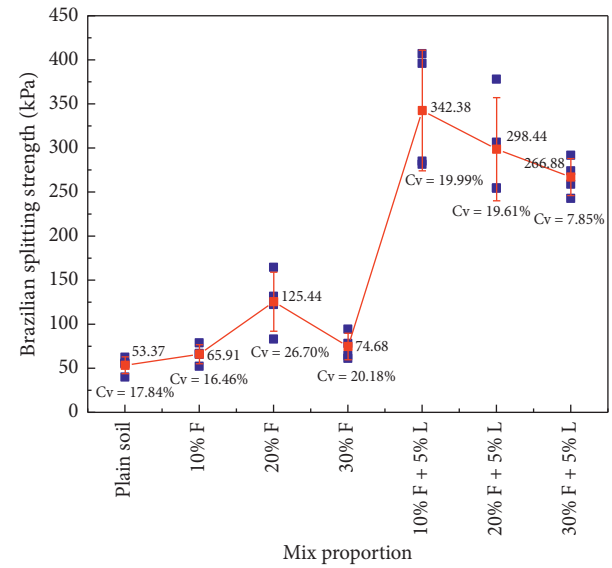

Figure 17: Brazilian splitting strength curve of stabilized soil (28 days).

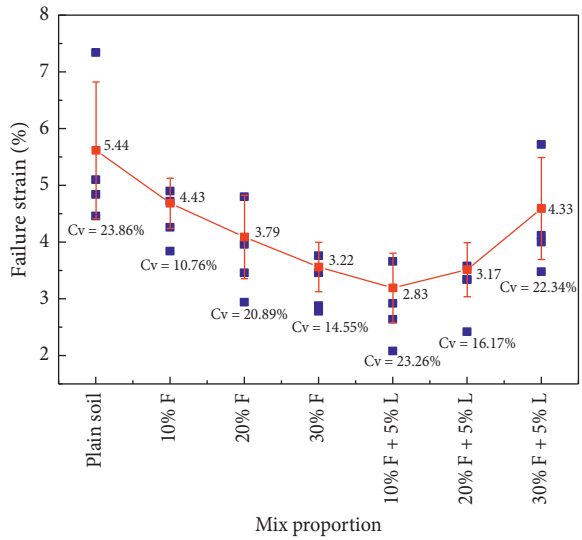

Figure 18: Brazilian splitting failure strain curve of stabilized soil (28 days).

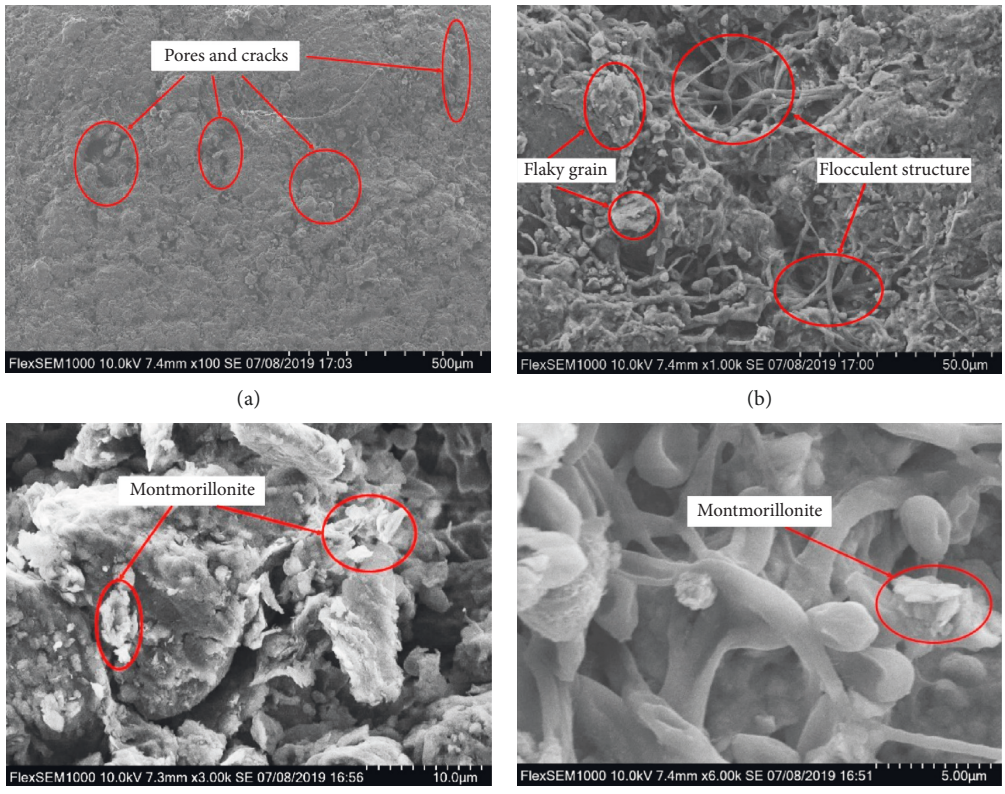

Figure 19: SEM images of plain soil under different magnification multiples (28 days). (a) ×100; (b) ×1000; (c) ×3000; (d) ×6000.

the fine pores or cracks are to some extent filled by the fly ash particles and hydration products. However, due to only small amount of hydration products, some fly ash particles have insufficient cementation with pores. Further enlargement of the images suggest that the fly ash hydration product (C-S-H) reacts with the clay particles. Thus, the original flaky soil particles are cemented into blocky structures, and the integrity of the soil particles is enhanced.

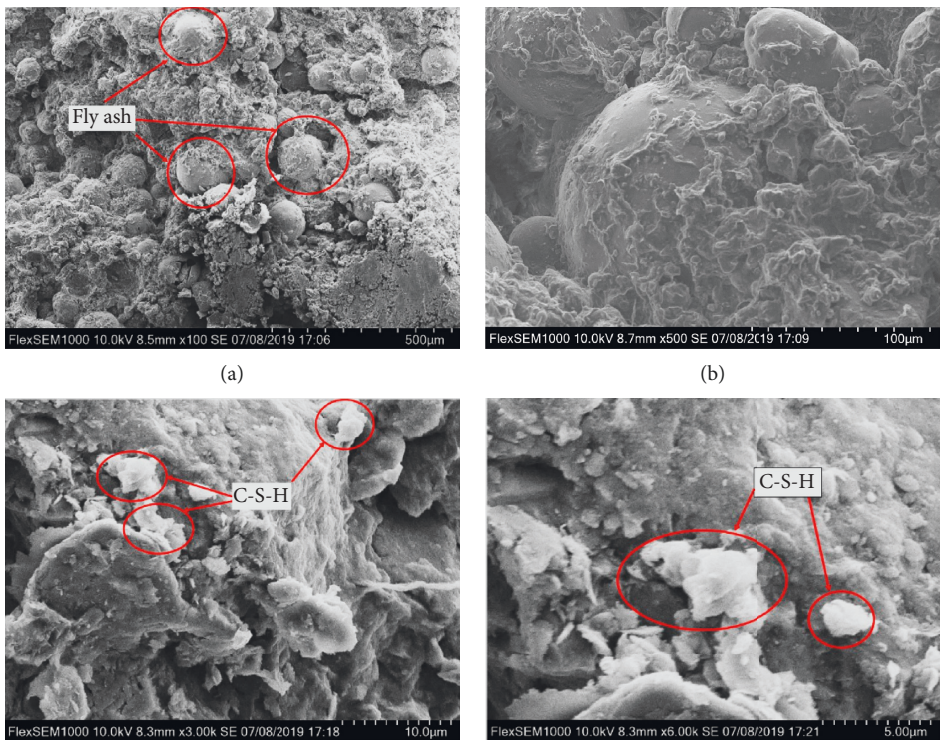

(a) (b) (c) (d)

Figure 20: SEM images of 10% F-modified expansive soil under different magnification multiples (28 days). (a) ×100; (b) ×1000; (c) ×3000; (d) ×6000.

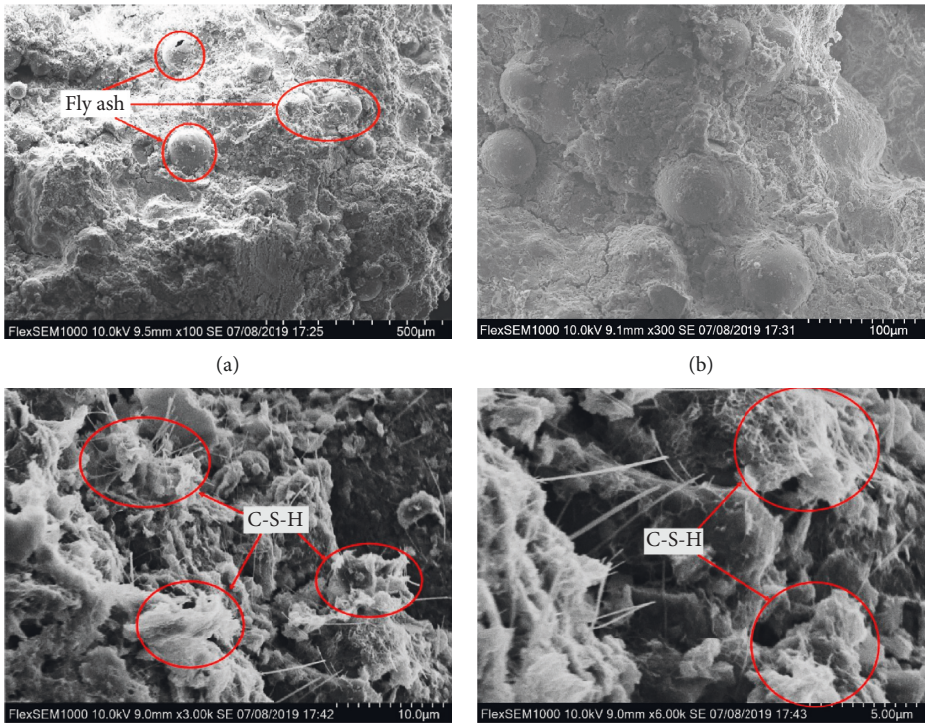

(a) (b) (c) (d)

Figure 21: SEM images of 10% F + 5% L-modified expansive soil under different magnification multiples (28 days). (a) ×100; (b) ×1000; (c) ×3000; (d) ×6000.

The structure of 10% F + 5% L-modified soil is found to be more compact, as shown in Figure 21. Hydration products produced by lime improve the degree of cementation between fly ash and the pores of plain soil, so fly ash particles are tightly embedded in the pores (a-b). Further enlarging the SEM image, it is suggested that the original flocculent structure and hydration products are cemented together (c-d), and the soil particles after the reaction form a crystal or blocky structure. At this time, the soil is no longer expansive.

3.3.2. XRD Results. The results of the XRD test are shown in Figure 22. The plain soil is found to be primarily composed of quartz, with a small amount of illite and montmorillonite. The major component of the soil modified by 10% F is a small amount of berlinite besides quartz. The main component of the soil after the modification of 10% F + 5% L is quartz, with a small amount of gismondine and berlinite. The comparison of the mineral components before and after the reaction is listed in Table 3.

The content of SiO_2 is downregulated significantly from 68.3253% (plain soil) to 62.4113% (10% F + 5% L). CaO content increases significantly from 0.8721% (plain soil) to 6.0566% (10% F + 5% L). Changes in mineral composition can be summed up as follows: for montmorillonite consists of two layers of Si-O tetrahedron and one layer Al-OH octahedron to constitute a 2 : 1 type crystal structure, which relies mainly on van der Waals force for connection between crystals. Al^{3+} in Al-OH octahedron is often replaced by other low cation such as Mg^{2+}, and Si^{4+} in Si-O tetrahedron is often replaced by Ca^{2+}. Therefore, extra negative charges appear between the crystals which can attract other cations (Na^+, K^+, etc.) and their hydration ions to fill between the crystals to form water film, thus enlarging the distance to achieve the purpose of expansion [40]. The schematic diagram is shown in Figure 23.

When fly ash and lime are added to expansive soil, the microstructures of clay (montmorillonite mainly) change greatly. The reason is that fly ash and lime react with water to form considerable Ca^{2+}. The relatively high-valent Ca^{2+} replaces K^+ and Na^+ in the clay particles via ion exchange to reduce the water film thickness of the soil particles. Simultaneously, the alkaline environment formed by the hydration of lime promotes the ion exchange. This is the main reason for reducing the swelling potential of soil. The relevant chemical reactions can be summarized as follows:

Ion exchange:

$$\mathrm{Na^+ - Al_2[Si_4O_{10}](OH)_2 \cdot nH_2O + Ca^{2+} \longrightarrow Ca^{2+} - Al_2[Si_4O_{10}](OH)2 \cdot nH_2O + Na^+} \quad (5)$$

The reason for the increase in strength of stabilized soil can be summarized that lime reacts with CO_2 in air to form a carbonaceous material for carbonizing the soil. The active

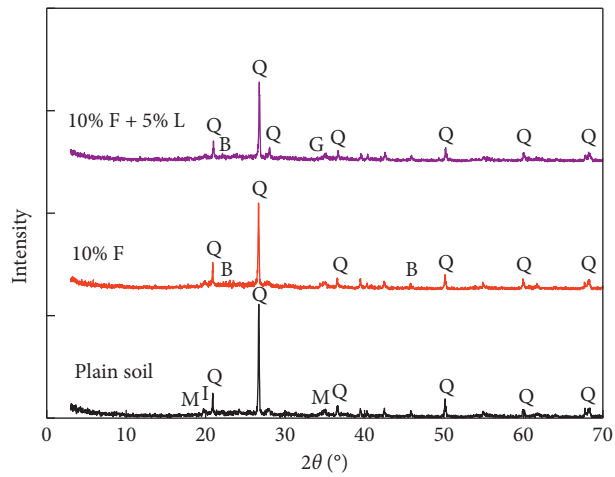

Q: quartz
I: illite
B: berlinite
G: gismondine
M: montmorillonite

Figure 22: XRD pattern of expansive soil.

Table 3: Comparison of mineral components.

Components	Result		
	(Plain soil) %	(10% F) %	(10% F + 5% L) %
SiO_2	68.3253	67.4133	62.4113
Al_2O_3	18.5417	20.3948	19.8111
Fe_2O_3	5.4264	5.0291	4.8851
K_2O	3.7010	3.3018	3.0552
MgO	1.2612	1.1262	1.5938
CaO	0.8721	0.9306	6.5056
TiO_2	0.7628	0.8181	0.8122
Na_2O	0.4421	0.4110	0.3432
MnO	0.1780	0.1483	0.1317
P_2O_5	0.1621	0.1233	0.1280
SO_3	0.0713	0.0904	0.1152

SiO_2 in clay particles reacts slowly with $Ca(OH)_2$ to form calcium silicate hydrate (C-S-H), which can both exist in water environment. The gel is produced and gradually transforms into fibrous crystals in the later stage. As the amount increases, the crystals cross each other to form a chain structure, thereby filling the particle pores to enhance the strength. The reaction formula is written as follows:

Carbonation:

$$\mathrm{Ca(OH)_2 + CO_2 \longrightarrow CaCO_3 + H_2O} \quad (6)$$

$$\mathrm{Mg(OH)_2 + CO_2 \longrightarrow MgCO_3 + H_2O} \quad (7)$$

Pozzolanic reaction:

$$\mathrm{Ca(OH)_2 + SiO_2 \longrightarrow CaO \cdot SiO_2 \cdot H_2O} \quad (8)$$

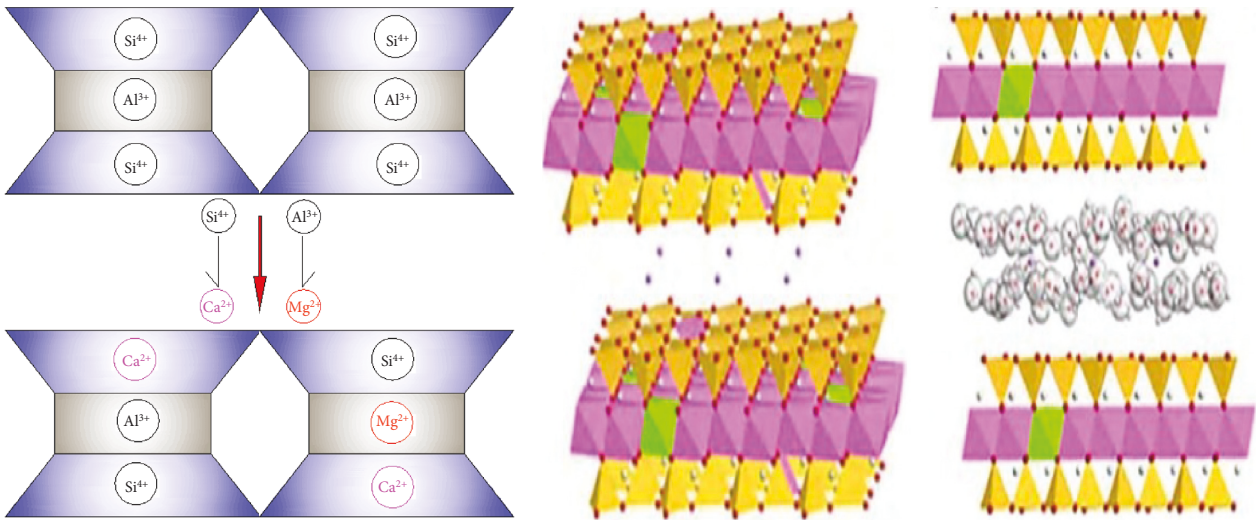

Figure 23: Schematic diagram of water absorption expansion in montmorillonite. (a) Ion exchange; (b) water absorption expansion.

4. Conclusion

This study first compared the physical and mechanical parameters of soil samples with different modifiers mix proportions. Then, three representative groups of soil samples were taken to perform SEM and XRD tests. Some major conclusions are drawn:

(1) The physical properties of modified soil are significantly different from those of plain soil. The PI, free swelling ratio, and unloading swelling ratio decrease slowly with the rise in fly ash content. After adding 5% lime, the PI, free swelling ratio, and unloading swelling ratio are significantly downregulated, suggesting that adding 5% lime based on fly ash can significantly reduce the expansion potential of expansive soil.

(2) The variation laws of unconfined compressive and tensile strengths of the stabilized soil have a consistency, which increase firstly and then decrease as fly ash content is upregulated. For pure fly ash stabilized soil, the unconfined compressive and tensile strengths reach the maximum under the conditions of 10% F and 20% F, respectively. When 5% lime is added based on 10% fly ash, the unconfined compressive and tensile strengths of the stabilized soil reache the peak value. The addition of lime can increase the hydration rate and enhance the early strength of stabilized soil. 10% F + 5%F is obtained as the optimal mix proportion.

(3) The microstructure and mineral composition analysis suggest that the plain soil is mostly in flaky and flocculent structures with obvious pores and cracks. The addition of fly ash makes the pores and cracks fill with fly ash particles and some hydration products. After the addition of lime, the ion exchange and pozzolanic reaction of lime makes the flaky and flocculent structures of soil cement into crystal or blocky structures, thereby enhancing the compactness and integrity of soil samples.

In this study, the stabilizing effects of fly ash and lime on the expansive soil were investigated and the optimal mixture ratio of the modifier was given. However, only two contents of lime (0%, 5%) were considered in the experiment, and other corresponding parameters like lime fixation point require further investigation.

Data Availability

The data used to support the findings of this study are available from the corresponding author upon request.

Conflicts of Interest

The authors declare that they have no conflicts of interest regarding the publication of this paper.

Acknowledgments

This work was supported by the Major Universities Natural Science Research Project in Anhui Province (KJ2016SD19) and the National Natural Science Foundation of China (41977236, 41672278, and 41271071). The authors sincerely thank the School of Civil Engineering and Architecture, National Engineering Laboratory for Deep Shaft Construction Technology in Coal Mine in Anhui University of Science and Technology, for providing the experiment conditions.

References

[1] J. Li, D. A. Cameron, and G. Ren, "Case study and back analysis of a residential building damaged by expansive soils," *Computers and Geotechnics*, vol. 56, pp. 89–99, 2014.

[2] H. H. Adem and S. K. Vanapalli, "Constitutive modeling approach for estimating *1-D* heave with respect to time for expansive soils," *International Journal of Geotechnical Engineering*, vol. 7, no. 2, pp. 199–204, 2013.

[3] T. M. Petry and D. N. Little, "Review of stabilization of clays and expansive soils in pavements and lightly loaded structures-history, practice, and future," *Journal of Materials in Civil Engineering*, vol. 14, no. 6, pp. 447–460, 2002.

[4] C. M. O. Nwaiwu and I. Nuhu, "Evaluation and prediction of the swelling characteristics of Nigerian black clays," *Geotechnical and Geological Engineering*, vol. 24, no. 1, pp. 45–56, 2006.

[5] A. R. Estabragh, M. Moghadas, and A. A. Javadi, "Effect of different types of wetting fluids on the behaviour of expansive soil during wetting and drying," *Soils and Foundations*, vol. 53, no. 5, pp. 617–627, 2013.

[6] H. H. Adem and S. K. Vanapalli, "Review of methods for predicting in situ volume change movement of expansive soil over time," *Journal of Rock Mechanics and Geotechnical Engineering*, vol. 7, no. 1, pp. 73–86, 2015.

[7] H. Elbadry, "Simplified reliable prediction method for determining the volume change of expansive soils based on simply physical tests," *HBRC Journal*, vol. 13, no. 3, pp. 353–360, 2017.

[8] P. VenkaraMuthyalu, K. Ramu, and G. V. R. Prasada Raju, "Study on performance of chemically stabilized expansive soil," *International Journal of Advances in Engineering & Technology*, vol. 2, no. 1, pp. 139–148, 2012.

[9] H. Zhao, K. Zhou, C. Zhao, B.-W. Gong, and J. Liu, "A long-term investigation on microstructure of cement-stabilized handan clay," *European Journal of Environmental and Civil Engineering*, vol. 20, no. 2, pp. 199–214, 2016.

[10] X. M. Li, M. S. Wang, and Y. H. Liang, "Study on treatment theory and technique for expansive soils geological disaster," in *Proceeding of the International Conference on Remote Sensing, Environment and Transportation Engineering (RSETE)*, pp. 802–806, IEEE, Nanjing, China, 2011.

[11] N. T. Skipper, P. A. Lock, J. O. Titiloye et al., "The structure and dynamics of 2-dimensional fluids in swelling clays," *Chemical Geology*, vol. 230, no. 3-4, pp. 182–196, 2006.

[12] K. Devineau, I. Bihannic, L. Michot et al., "In situ neutron diffraction analysis of the influence of geometric confinement on crystalline swelling of montmorillonite," *Applied Clay Science*, vol. 31, no. 1-2, pp. 76–84, 2006.

[13] J. C. Jia, *Study on the swelling mechanism and mesomechanical swelling model of expansive soils*, Ph.D. thesis, Dalian University of Technology, Dalian, China, 2010.

[14] Z. Z. Ding, Y. R. Zheng, and L. S. Li, "Trial study on variation regularity of swelling force," *Rock and Soil Mechanics*, vol. 28, no. 7, pp. 1328–1332, 2007, in Chinese.

[15] X. N. Cui, Q. C. Wang, R. L. Zhang, J. Q. Li, and B. Z. Wang, "Principal component analysis-based prediction of swelling force of expansive soil," *Water Resources and Hydropower Engineering*, vol. 49, no. 7, pp. 181–186, 2018, in Chinese.

[16] P. Samui, S. K. Das, and T. G. Sitharam, "Application of soft computing techniques to expansive soil characterization," in *Intelligent and Soft Computing in Infrastructure Systems Engineering*, vol. 259, pp. 305–323, Springer Nature, Basel, Switzerland, 2009.

[17] J. P. Quirk and S. Marčelja, "Application of double-layer theories to the extensive crystalline swelling of Li-montmorillonite," *Langmuir*, vol. 13, no. 23, pp. 6241–6248, 1997.

[18] D. Laird and C. Shang, "Relationship between cation exchange selectivity and crystalline swelling in expanding 2:1 phyllosilicates," *Clays and Clay Minerals*, vol. 45, no. 5, pp. 681–689, 1997.

[19] T. Leng, C. S. Tang, D. Xu et al., "Advance on the engineering geological characteristics of expansive soil," *Journal of Engineering Geology*, vol. 26, no. 1, pp. 112–128, 2018, in Chinese.

[20] M. Ito and S. Azam, "Engineering properties of a vertisolic expansive soil deposit," *Engineering Geology*, vol. 152, no. 1, pp. 10–16, 2013.

[21] Z. Q. Li, W. L. Yu, L. Fu et al., "Research on expansion and contraction rules and disaster mechanism of expansive soil," *Rock and Soil Mechanics*, vol. 31, no. 2, pp. 270–275, 2010, in Chinese.

[22] R. N. Yong and V. R. Ouhadi, "Experimental study on instability of bases on natural and lime/cement-stabilized clayey soils," *Applied Clay Science*, vol. 35, no. 3-4, pp. 238–249, 2007.

[23] A. S. Rao and M. R. Rao, "Swell-shrink behaviour of expansive soils under stabilized fly ash cushions," in *Proceedings of the 12th International Conference on International Association for Computer Methods and Advances in Geomechanics*, pp. 561–564, Goa, India, December 2008.

[24] B. A. Mir, "Some studies on the effect of fly ash and lime on physical and mechanical properties of expansive clay," *International Journal of Civil Engineering*, vol. 13, no. 3-4, pp. 203–212, 2015.

[25] B. Bose, "Geo-engineering properties of expansive soil stabilized with fly ash," *EJGE*, vol. 17, pp. 1339–1353, 2012.

[26] A. K. Sabat, "A study on some geotechnical properties of lime stabilized expansive soil-quarry dust mixes," *International Journal of Emerging Trends in Engineering and Development*, vol. 1, no. 2, pp. 42–49, 2012.

[27] X. Y. He, Y. M. Chen, W. S. Zhang, Y. X. Li, H. T. Zhang, and R. Tang, "Research and development of chemical consolidation of expansive soil," *Journal of the Chinese Ceramic Society*, vol. 31, no. 11, pp. 1101–1106, 2003, in Chinese.

[28] Y. X. Wang, P. P. Guo, S. B. Shan, Y. L. Qian, and W. K. Lu, "Experimental research and micromechanism analysis for expansive soil of Hefei improved by cation," *Industrial Construction*, vol. 45, no. 9, pp. 104–109, 2015, in Chinese.

[29] F. S. Zha, S. Y. Liu, and Y. J. Du, "Experiment on improvement of expansive clays with lime-fly ash," *Journal of Southeast University*, vol. 37, no. 2, pp. 339–344, 2007, in Chinese.

[30] P. V. Sivapullaiah and A. K. Jha, "Gypsum induced strength behaviour of fly ash-lime stabilized expansive soil," *Geotechnical and Geological Engineering*, vol. 32, no. 5, pp. 1261–1273, 2014.

[31] P. S. Parhi, L. Garanayak, M. Mahamaya, and S. K. Das, "Stabilization of an expansive soil using alkali activated fly ash based geopolymer," in *Advances in Characterization and Analysis of Expansive Soils and Rocks*, pp. 36–50, Springer Nature, Basel, Switzerland, 2017.

[32] Y. J. Li, L. Li, and H. C. Dan, "Study on application of TerraZyme in road base course of road," *Applied Mechanics and Materials*, vol. 97-98, pp. 1098–1108, 2011.

[33] H. Ye, C. Chu, L. Xu, K. Guo, and D. Li, "Experimental studies on drying-wetting cycle characteristics of expansive soils improved by industrial wastes," *Advances in Civil Engineering*, vol. 2018, Article ID 2321361, 9 pages, 2018.

[34] J. James, P. K. Pandian, and A. S. Switzer, "Egg shell ash as auxiliary addendum to lime stabilization of an expansive soil," *The Journal of Solid Waste Technology and Management*, vol. 43, no. 1, pp. 15–25, 2017.

[35] C. Kennedy, T. O. Amgbara, and T. T. T. Wokoma, "Comparative evaluation of effectiveness of cement/lime and Costus afer bagasse fiber stabilization of expansive soil," *Global Scientific Journals*, vol. 6, no. 5, pp. 97–110, 2018.
[36] Ministry of Construction of the People's Republic of China, *GB/T 50123–1999 Standard for Soil Test Method*, China Planning Press, Beijing, China, 1999, in Chinese.
[37] A. Tavallali and A. Vervoort, "Effect of layer orientation on the failure of layered sandstone under Brazilian test conditions," *International Journal of Rock Mechanics and Mining Sciences*, vol. 47, no. 2, pp. 313–322, 2010.
[38] D. Q. Dan, H. Konietzky, and M. Herbst, "Brazilian tensile strength tests on some anisotropic rocks," *International Journal of Rock Mechanics and Mining Sciences*, vol. 58, pp. 1–7, 2013.
[39] C. D. Ding, D. W. Hu, H. Zhou, J. J. Lu, D. D. Ma, and Y. Zhang, "Brazilian splitting tests of slate considering three-dimensional foliation effect," *Chinese Journal of Rock Mechanics and Engineering*, vol. 38, no. 2, pp. 301–312, 2019, in Chinese.
[40] H. Zhao, S. Jiang, Y. Ge, and C. Liu, "Molecular dynamics simulation of water molecules adsorption by different cations based montmorillonite," *Scientia Sinica Technologica*, vol. 49, no. 6, pp. 703–715, 2019, in Chinese.